EARTHQUAKE ENGINEERING AND STRUCTURAL DYNAMICS, VOL. 25, 509–526 (1996)

DYNAMIC CROSS-INTERACTION BETWEEN FLEXIBLE SURFACE FOOTINGS BY COMBINED BEM AND FEM

J. QIAN, L. G. THAM AND Y. K. CHEUNG
Department of Civil and Structural Engineering, Hong Kong University, Hong Kong

SUMMARY

A combined boundary and finite element method is developed and applied to study the dynamic behaviour of a system of flexible surface footings of arbitrary shape bearing on an elastic half-space. The proposed method employs the frequency domain Green's function for the surface of the elastic half-space while a layered plate model is used for the flexible footing. Both the footing and the surface of the half-space are discretized by 8-noded quadratical isoparametric elements, and the meshes are identical. Thus, the compatibility of displacements and equilibrium of forces between the footing and the half-space are fully satisfied. This model provides a better approximation of the stress concentration at edges of relatively rigid footings. Numerical examples demonstrating the effects due to the excitation frequency, the relative rigidity and the distance between footings on the interaction between two square footings are presented. The external forces can be either harmonic or transient.

KEY WORDS: dynamic soil–structure interaction; surface footing; boundary and finite element methods

1. INTRODUCTION

Many studies have been conducted to investigate the dynamic interaction between the soil and structure and the interaction through the soil between adjacent structures as well. Apparently, Warburton *et al.*[1] were the first to study the problem of dynamic cross-interaction between two circular massive foundations subjected to external forces. Dominguez[2] proposed a frequency domain boundary element method to solve the problem of foundation dynamics. A number of review-type articles[3, 4] and the author's previous work[5] have provided an up-to-date literature survey on the subject. In most cases of dynamic interaction analysis, structures were assumed to be founded on mat foundations or interconnected footings and they were considered to be infinitely rigid.[1, 5] Although it has been noted that the assumption of a rigid footing may not always be valid,[6, 7] only a few papers have addressed the problem of the effects of footing flexibility on their dynamic behaviour.

Oien[8] analysed the response of a flexible strip in smooth contact with the elastic half-space subjected to obliquely incident harmonic waves by using the Bubnov–Galerkin method. The same problem was later investigated by Spyrakos and Beskos[9] employing a time-domain boundary element method in conjunction with finite element discretization for the flexible strip footing. Savidis and Richter[10] studied the effects of the flexibility of rectangular footings on their response to external forces. The variations of the dynamic contact pressure as well as the vertical displacement were plotted against the dimensionless frequency but their results were limited to the lower-frequency range. An extensive parametric study was presented by Whittaker and Christiano for a plate on the elastic half-space subject to harmonic waves[11] as well as to harmonic time-varying external forces.[12] The dynamic responses of a square flexible footing with a rigid perimeter or with a rigid core have been obtained by Iguchi and Luco.[7] In all these studies,[7, 10–12] the footing was modelled by finite elements while the half-space was modelled by boundary elements with the assumption of constant contact pressure within each surface element. Karabalis *et al.*[13, 14] proposed a time-domain boundary element method in combination with the finite element method for a flexible footing to study the dynamic response of a three-dimensional problem. In general, those numerical methods can provide results

CCC 0098–8847/96/050509–18

Received 17 October 1995
Revised 2 January 1996

of sufficient accuracy from the view point of the force–displacement relationship. However, they may not be detailed enough to study the variation of contact stresses beneath the footings as the assumption of constant pressure within each discretized subregion has been adopted. Analytical procedures may provide a more precise view into the problem, though they are usually restricted to cases of simple geometry. Lin[15] studied a circular plate with a rigid perimeter resting on a viscoelastic half-space by using an integral equation approach. Results for an elastic circular plate on a half-space were presented by Krenk and Schmidt.[16] Iguchi and Luco[6] studied again a circular plate with a rigid core. The dynamic response of annular plates on a viscoelastic half-space was obtained by Rajapakse.[17]

Concerning cross-interaction between adjacent flexible footings, it seems that the study carried out by Wang *et al.*[18] is the only one on the subject. In Wang's work, a coupled variational-Green's function scheme is employed to investigate the dynamic interaction between flexible strip footings.

In this paper the frequency domain boundary element method in association with the half-space Green's function and quadratic quadrilateral elements discretization[5] is extended to study the interaction effects between a system of flexible footings. The flexible footing is described by a layered plate model. This model is equivalent to the Reissner's or Mindlin's plate theory and is proved to be ideally suited for the contact problem[19, 20] in which case stress concentrations may occur along the edges of the contact region. The same 8-noded quadrilateral element is employed to discretize the surface of the half-space as well as the flexible footings and thus compatibility of displacements and equilibrium of forces are fully satisfied at the contact interfaces. Numerical results for two square footings are presented to demonstrate the effects of the flexibility of footings on their dynamic behaviour.

2. FREQUENCY-DOMAIN FORMULATION

2.1. BEM formulation for the elastic half-space

The boundary element method (BEM) is well-suited for the problem concerned because of its ability to model infinite media. A number of BEM formulations for the soil impedance matrix have been developed by several researchers for this purpose. In the frequency domain, if the surface half-space Green's function is employed, the surface displacement due to any stress distribution on the surface of the half-space can be calculated by using the following integral representation:[5]

$$u_i = \int_{S_f} G_{ij}(x - x_p, y - y_p, 0)\, t_j(x_p, y_p, 0)\, ds \tag{1}$$

where G_{ij} is the surface half-space Green's function or Lamb's displacement tensor[5] for the surface displacement in the ith direction at $(x, y, 0)$ due to a unit force acting in the jth direction at $(x_p, y_p, 0)$. The explicit form of G_{ij} is given in the Appendix.

For the numerical solution of equation (1), the soil-footing interface S_f is discretized into a number of 8-noded quadratic isoparametric boundary elements. It has been shown that this quadratic representation has advantages not only with respect to its higher accuracy and rapid convergence, but also for its ability to accommodate complex geometries.[5, 21, 22] Thus, equation (1) is transformed into the discretized form

$$\{U_s\} = [G]\{T_s\} \tag{2}$$

where $\{U_s\}$ and $\{T_s\}$ denote the nodal values of displacements and tractions respectively. The detailed derivation of the influence matrix $[G]$ can be found elsewhere.[5]

2.2. FEM formulation for flexible footings

A layered model is used to calculate the deformation of the flexible plate. The 8-noded element which has exactly the same plan geometry and interpolation of field variable as that used in the BEM discretization is

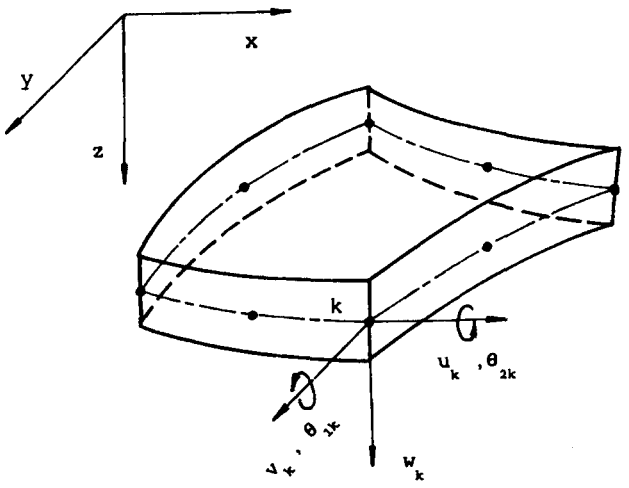

Figure 1. The 8-noded finite element for a flexible footing

adopted. Five degrees of freedom, as shown in Figure 1, are specified at each nodal point, corresponding to its three displacements and two rotations. The definition of independent rotation and displacement degrees of freedom permits transverse shear deformation to be taken into account. Thus this model is valid not only for the classical thin plate but also for the moderately thick one of Reissner's or Mindlin's type.

The element displacement field can then be expressed by

$$\{U\} = [N]\{\delta\} \tag{3}$$

where $\{\delta\}$ is the vector of element nodal variables and $[N]$ the shape function matrix.

$$\{\delta\} = \{u_k, v_k, w_k, \theta_{1k}, \theta_{2k}\}^T$$

The final finite element equation describing the behaviour of a flexible plate takes the form

$$[K]\{\delta\} = \{F\} \tag{4}$$

where $[K]$ is the global stiffness matrix and $\{\delta\}$ is the nodal displacement vector. The total nodal force vector $\{F\} = \{P\} + \{R\}$ is composed of two parts, the external force $\{P\}$ and the contact force $\{R\}$ which can be expressed in terms of the nodal values of tractions at the soil-footing interface

$$\{R\} = [H]\{T_f\} \tag{5}$$

where $\{T_f\}$ is the nodal values of tractions on the soil-footing interface and the transform matrix $[H]$ is assembled from element matrices $[H]^e$ of the form

$$[H]^e = \int_{S_f^e} [N]^T [N]\, ds \tag{6}$$

2.3. Combination of BEM and FEM for dynamic response analysis

Since the same 8-noded quadratic quadrilateral elements are employed for the discretization of the soil medium and flexible footing, as shown in Figure 2, the compatibility conditions at the soil-footing interface can be easily described by nodal values as

$$\{U_s\} = \{U_f\} \tag{7}$$

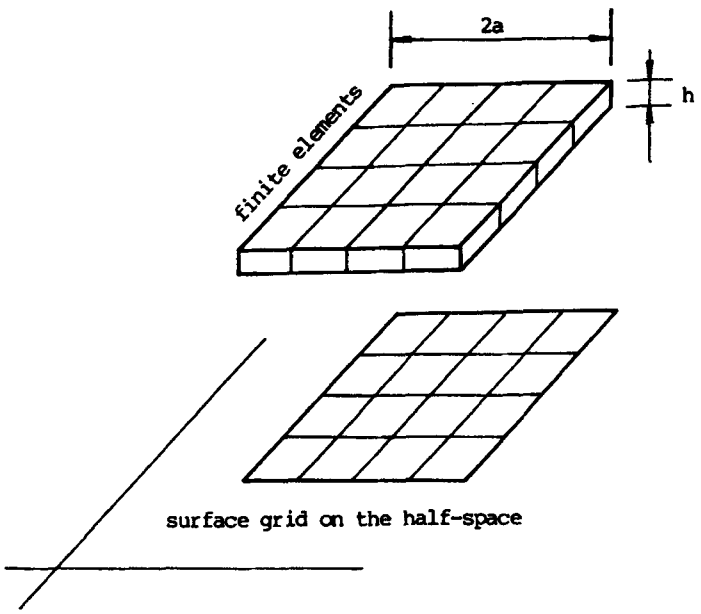

Figure 2. Discretization of a 3-D flexible surface footing

The vector $\{U_f\} = \{u_k, v_k, w_k\}^T$ contains three displacement components at each node. The equilibrium at the interface now reads

$$\{T_s\} = -\{T_f\} \tag{8}$$

The combination of equations (1), (4), (7) and (8) results in

$$([\bar{K}][G] + [H]\{T_s\} = \{P\} \tag{9}$$

where the bar indicates the stiffness matrix of the flexible footings after condensation. The approach adopted follows the way of the static condensation so that the rotational degrees of freedom will be eliminated from the re-assembled linear algebraic equations. Once the above equation is solved for $\{T_s\}$, $\{U_s\}$ is found with the aid of equation (2).

3. INFLUENCE OF FOOTING FLEXIBILITY ON DYNAMIC RESPONSE

To test the validity of the proposed method, a square footing of side $2a$ and thickness h subjected to either central point load P or to uniform load q is analysed. The stiffness of the footing is expressed through the relative rigidity E defined as

$$E = \frac{1}{12}\frac{E_f}{E_s}\left(\frac{h}{a}\right)^3$$

where E_s and E_f are Young's modulus of the soil and the footing, respectively. In all cases studied in this section and the following section, the dimensionless thickness of the footing h/a is taken to be 1/10.

Figure 3 shows the dimensionless vertical displacement amplitude Δ under a central point load versus the dimensionless excitation frequency ω_0 for three points on the footing: centre, midway along an edge, and

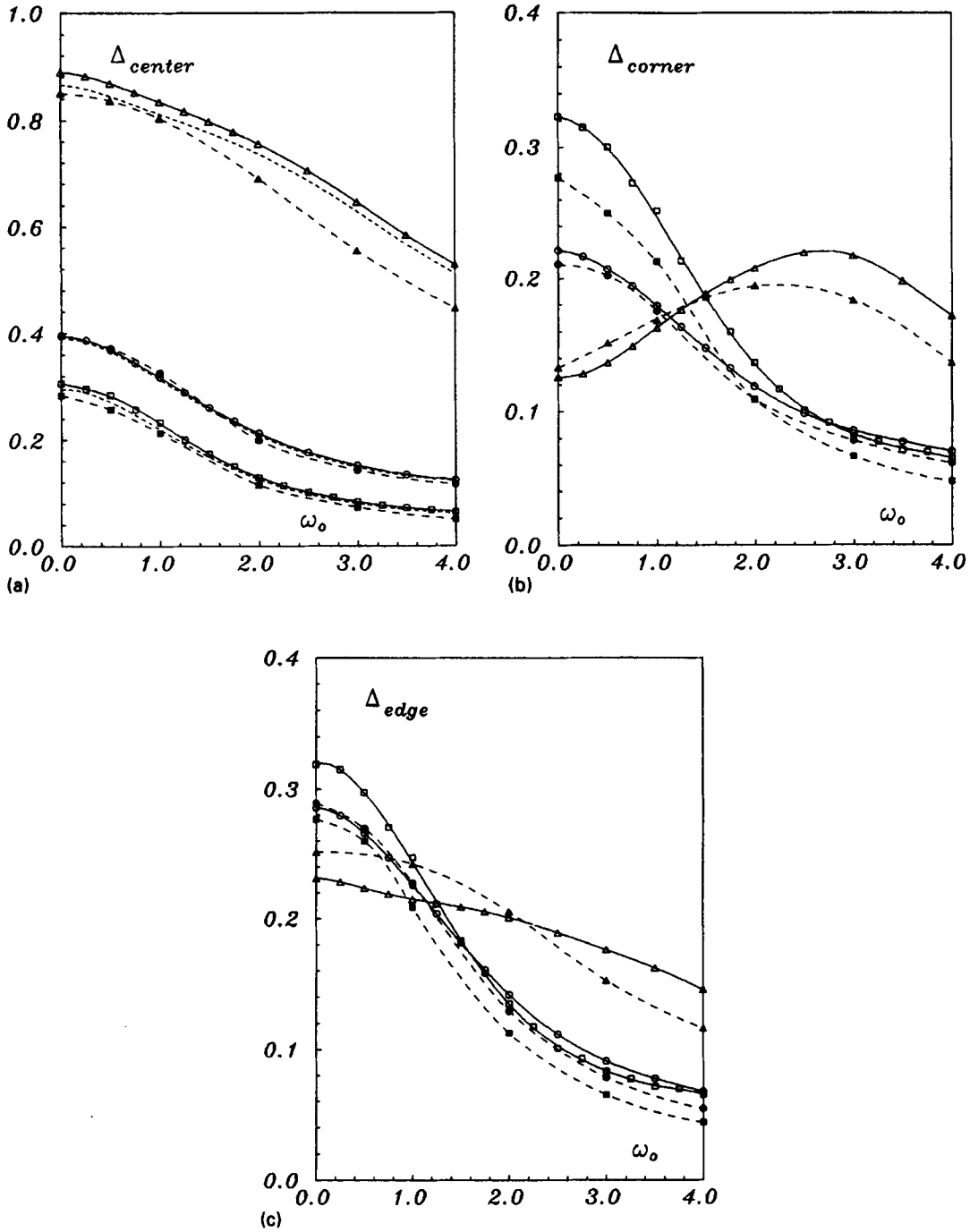

Figure 3. Vertical amplitude at (a) the centre, (b) a corner, and (c) the mid-point of an edge due to a central point load: (———) 8 × 8 BEM; (·····) 4 × 4 BEM; (– – – –) Whittaker *et al.*;[12] (△, ▲) $E_1 = 0{\cdot}016$; (⊙ ●) $E_2 = 0{\cdot}240$; (□ ■) $E_3 = 13{\cdot}2$

corner. Those dimensionless parameters are defined as

$$\Delta = aE_s|W|/P(1 + v_s)$$

$$\omega_0 = \omega a/c_s$$

in which c_s is the shear wave velocity of the soil. The Poisson's ratios for the soil v_s and for the footing v_f are taken to be 0.30. The footing is discretized by 4×4 and 8×8 elements and 6 layers along its thickness. Numerical tests indicate that a 6-layer discretization is accurate enough to describe the bending behaviour of a plate of moderate thickness. It has been tested that the proposed method converges very rapidly. As an example, Figure 3(a) shows that results obtained by 4×4 elements (broken lines without symbols) are very close to those corresponding results obtained by a refined 8×8 mesh (solid lines with symbols for three different plate rigidities). Differences between the two sets of results are within a few percent. It is also observed in Figure 3 that results calculated by the proposed method are in very good agreement with those of Whittaker and Christiano[12] at the centre point. Results of Whittaker and Christiano[12] were obtained by assuming constant contact pressure within each element and with a 64 element discretization. In practice, a footing with $E > 1{\cdot}0$ can be considered as a rigid one, and the discrepancy only appears in the two sets of results at the edge and corner points of the flexible footings. Although both the formulation of Whittaker and Christiano[12] and the one presented here employ a finite element characterization for the footing and the integral representation for the elastic half-space, the conditions of compatibility at the contact interface are imposed in a different fashion. In Reference 12, three generalized nodal displacements of the footing were defined at the corners of a quadrilateral element while displacements and contact stresses for the half-space were defined at the centroid of each subregion. To impose the compatibility of deformation for the footing and the half-space, two different discretization meshes for the footing and the half-space were employed so that two sets of nodal points coincided with each other. Thus the conditions of compatibility were imposed at nodes only. Similar treatment has also been used by Savidis and Richter[10] and Karabalis *et al.*[14] It was also pointed out by Iguchi and Luco[7] that such treatment had effectively averaged the contact stresses for each subregion, and they suggested that the use of mean values at corner nodes may lead to a better result. In the present work, fully consistent discretization is used and thus it is believed that the results presented here should be more accurate than those presented in Reference 12.

The same trend is again observed in Figure 4 for the case of the vertical response amplitude, $\Delta = E_s|W|/aq(1 + v_s)$, under a uniformly distributed load q per unit area. It is interesting to note that the responses computed by the present method and those by Whittaker and Christiano[12] for a footing with moderate rigidity $E = 0{\cdot}24$ are always in excellent agreement at all the three points concerned.

The static contact pressure of a square footing under uniform load is calculated and compared with that of Cheung and Zienkiewicz[23] for five values of relative rigidity E. In this case, the Poisson's ratios for both the soil and the footing are taken to be $v_s = v_f = 1/3$. In Reference 23, one quadrant of the footing was discretized by 3×3 finite elements and the flexibility matrix of the half-space was calculated by using the Boussinesq equation in conjunction with the assumption of constant contact pressure over each element. Figure 5 shows the normalized contact pressure σ_{zz}/q along a centre line of the footing obtained by an 8×8 quadratic element and 6-layer discretization. The results indicate that the contact pressure would converge to the uniform loading when the relative rigidity of the footing approaches zero. It is also observed that the stress concentration at the edges becomes more pronounced as the stiffness of the footings increases. The apparent difference in the contact pressure between the two sets of results can be explained by the fact that Reference 23 started off with the assumption of constant contact pressure over each subregion and that each curve presented actually represented a line connecting centroidal stresses.

4. DYNAMIC CROSS-INTERACTION BETWEEN TWO FLEXIBLE SQUARE FOOTINGS

The dynamic response of two identical square footings, shown in Figure 6, of side $2a$ and thickness h resting on the half-space with a Poisson's ratio $v_s = 1/3$ is considered in this section. The two footings are placed side by side with a centre-to-centre distance d. The Poisson's ratio for the footing is $v_f = 0{\cdot}30$. A 6×6 element and 6-layer discretization is employed for both the active footing, which is subjected to an external excitation force, and the passive footing which is load-free. Four values of relative rigidity are considered: $E_1 = 1{\cdot}745$, $E_2 = 0{\cdot}1458$, $E_3 = 0{\cdot}02431$ and $E_4 = 0{\cdot}007794$.

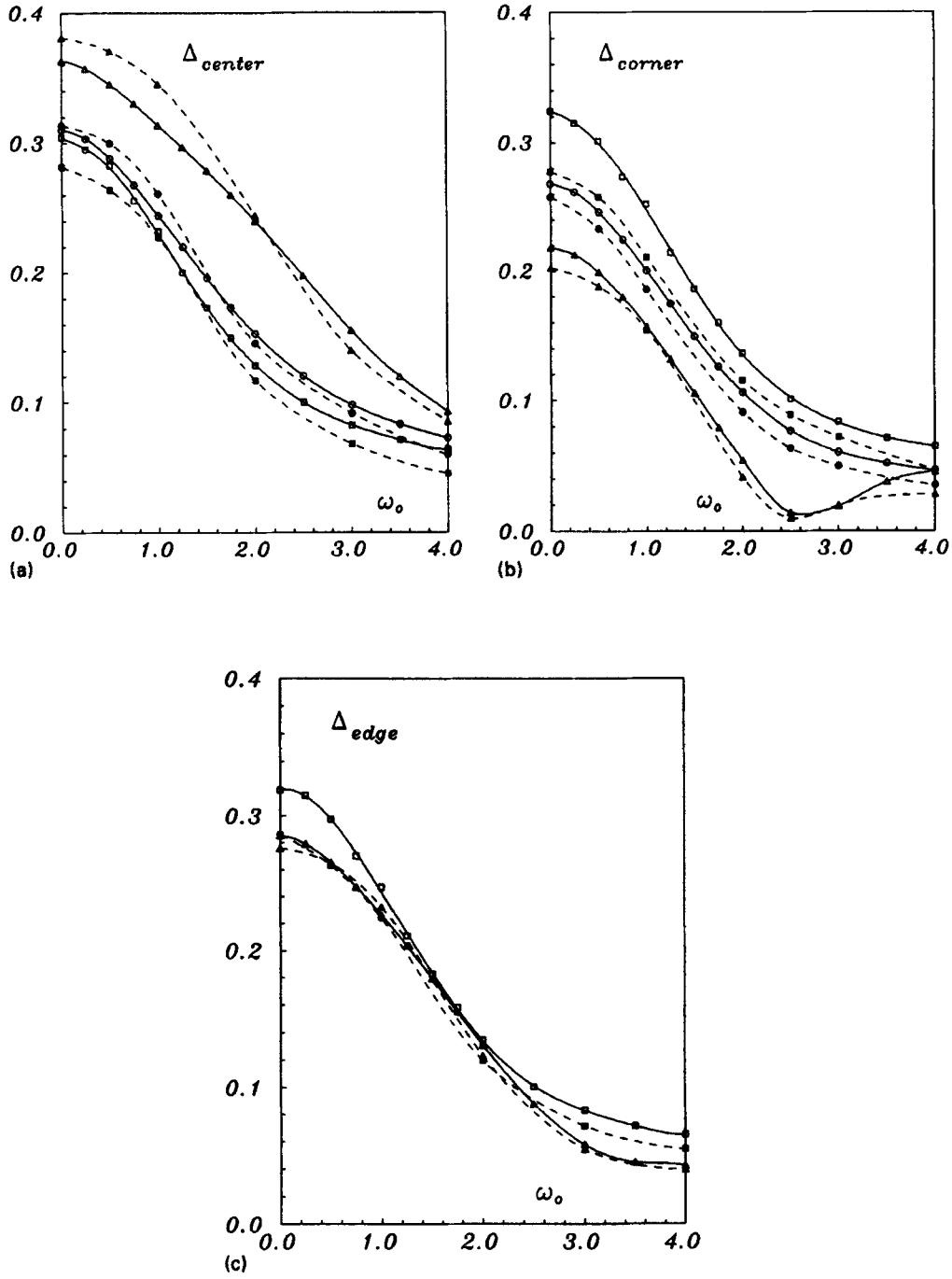

Figure 4. Vertical amplitude at (a) the centre, (b) a corner, and (c) the mid-point of an edge due to a uniformly distributed load: (———) 8 × 8 BEM; (·····) 4 × 4 BEM; (– – – –) Whittaker *et al.*;[12] (△, ▲) $E_1 = 0{\cdot}016$; (⊙ ●) $E_2 = 0{\cdot}240$; (□ ■) $E_3 = 13{\cdot}2$

The vertical compliance function C_{ij} for the active footing under a central point load P_i is shown in Figure 7, where, $C_{ij} = aE_sW_j/2P_i(1 + v_s)$, subscripts i and j, $i, j = 1, 2, \ldots, 6$, indicate the locations of excitation and response, respectively, and are defined for the two footings in Figure 6. Results denoted by $1F$ represent the calculated values for a single footing. It is interesting to note that the influence of the load-free second footing

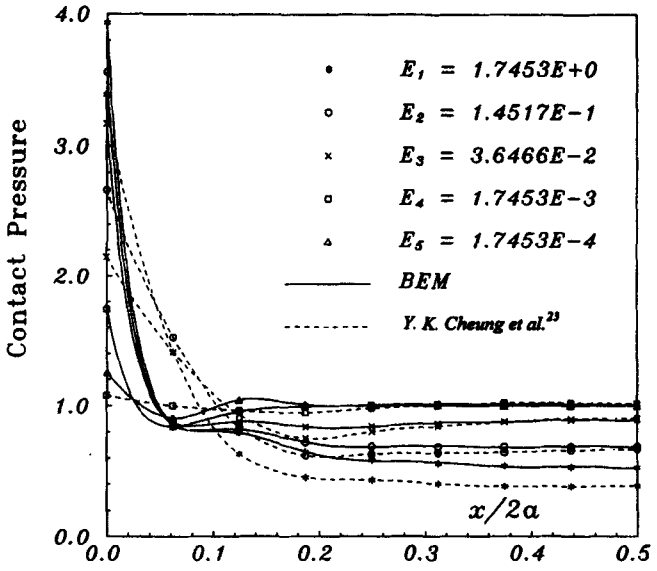

Figure 5. The normalized static contact pressure of a square footing σ_{xx}/q

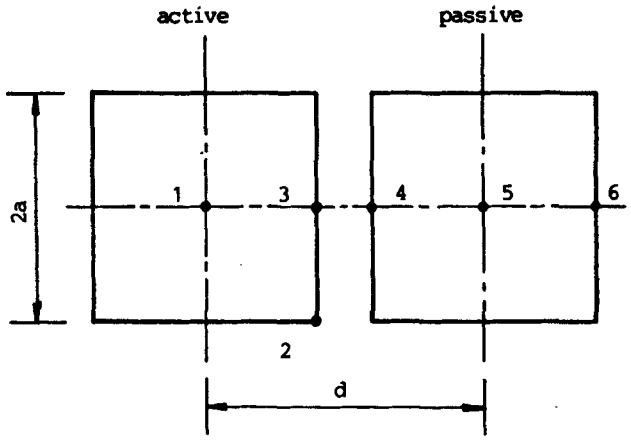

Figure 6. The two square footing system

on the compliance function of the active footing is very small. Detailed numerical studies, shown in Figure 8, indicate that its effect seems negligible for any finite values of footing separation. Again, similar to the situation shown in the previous section for a single footing, the compliance at the centre of a soft footing may be several times that of a stiff one. With increasing footing rigidity, the calculated values approach the results for a rigid footing obtained by Rizzo *et al.*[22]

The coupling will generate contact forces as well as displacements on the passive footing. The coupling compliance functions at three points on the centre line of the passive footing are given in Figures 9–11 for the dimensionless separation distance $d/a = 2{\cdot}5, 5{\cdot}0, 10$, respectively. It has been shown that the amplitude of the coupling compliance function decreases with increasing separation distance d. For relatively rigid foundations, it decays rapidly at higher frequency and it seems that there is a 'threshold frequency' beyond which no significant displacements to the load-free footing will be generated by the adjacent excitation. The value of the 'threshold frequency' decreases with increasing footing separation. For soft footings, there is no evidence

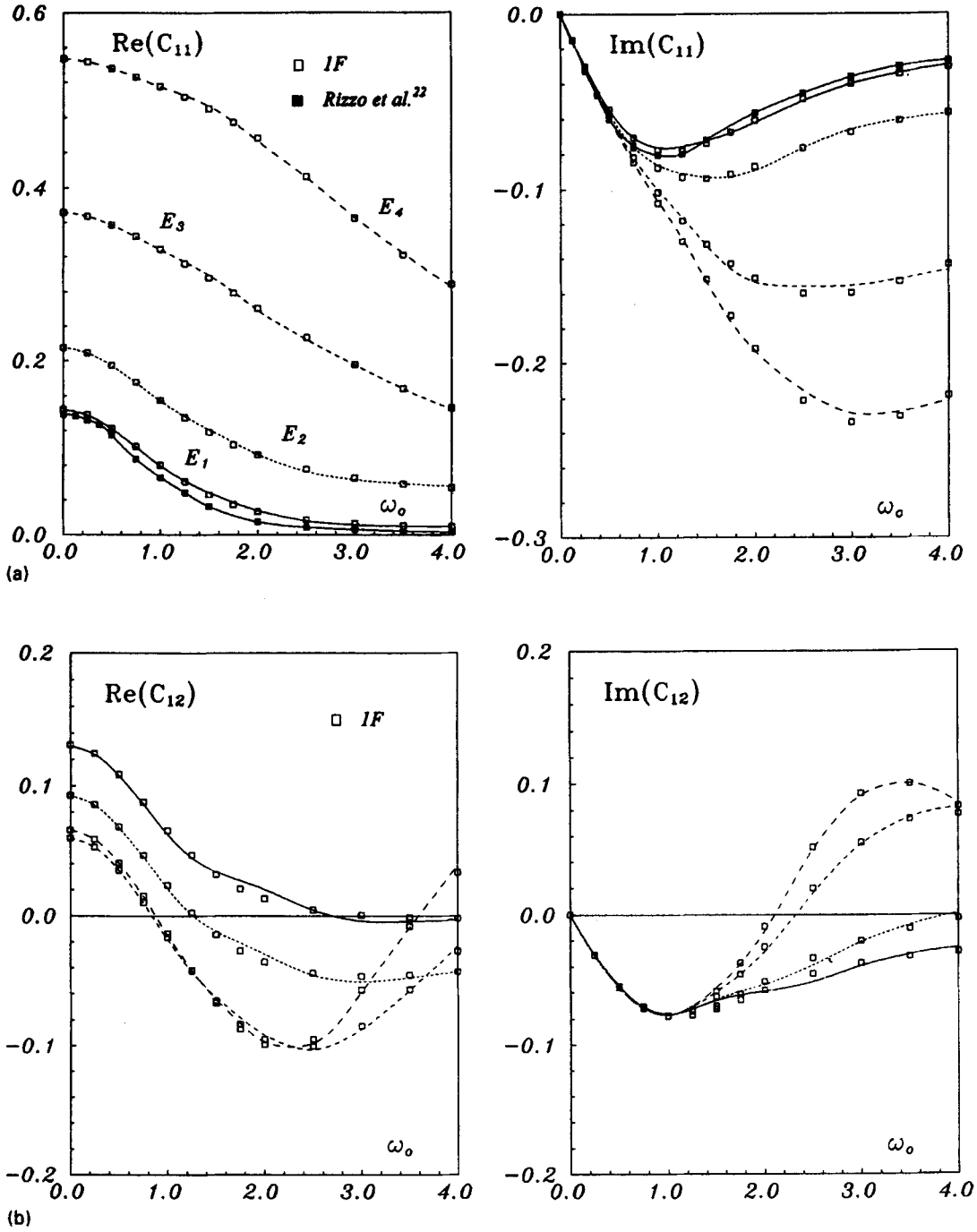

Figure 7. Vertical compliance of the active footing at (a) the centre, (b) corner No. 2, and (c) mid-point of an edge, No. 3 for footing separation $d/a = 2{\cdot}50$: (———) E_1; (· · · · ·) E_2; (– – – –) E_3; (— — —) E_4

that the coupling compliance function has declined in its amplitude within the concerned frequency range. It behaves in an oscillatory pattern.

The vertical compliance function, $C_{1j} = E_s W_j / 2aq(1 + v_s)$, for the same footing system subjected to a uniform load are presented in Figures 12 and 13. Figure 12 shows the compliance function for the active

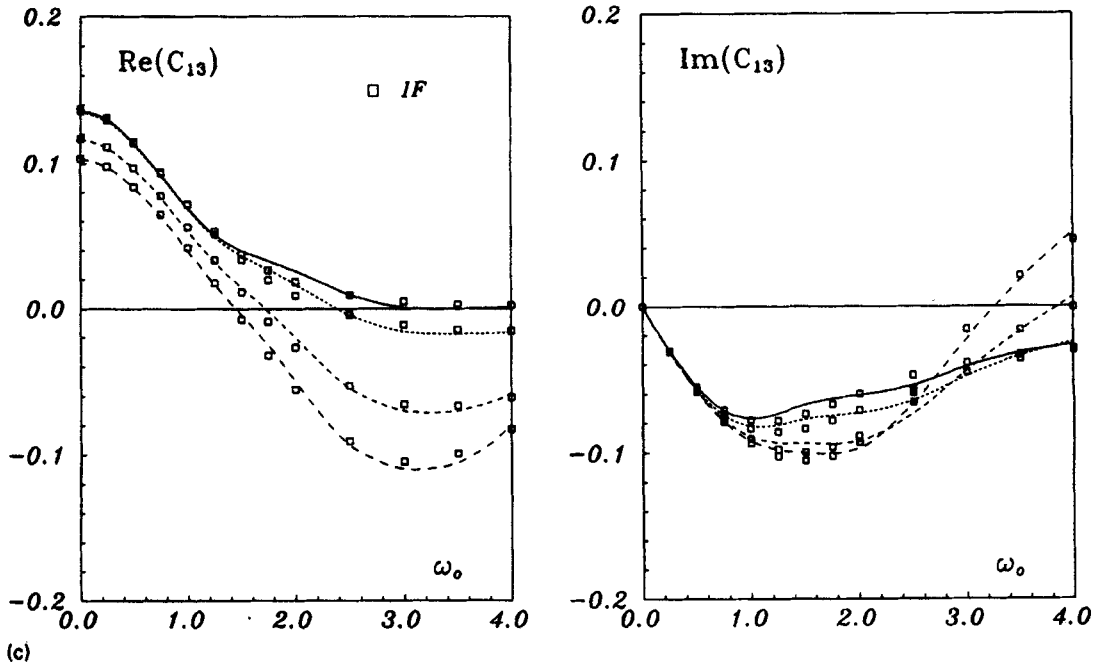

Figure 7. *Continued*

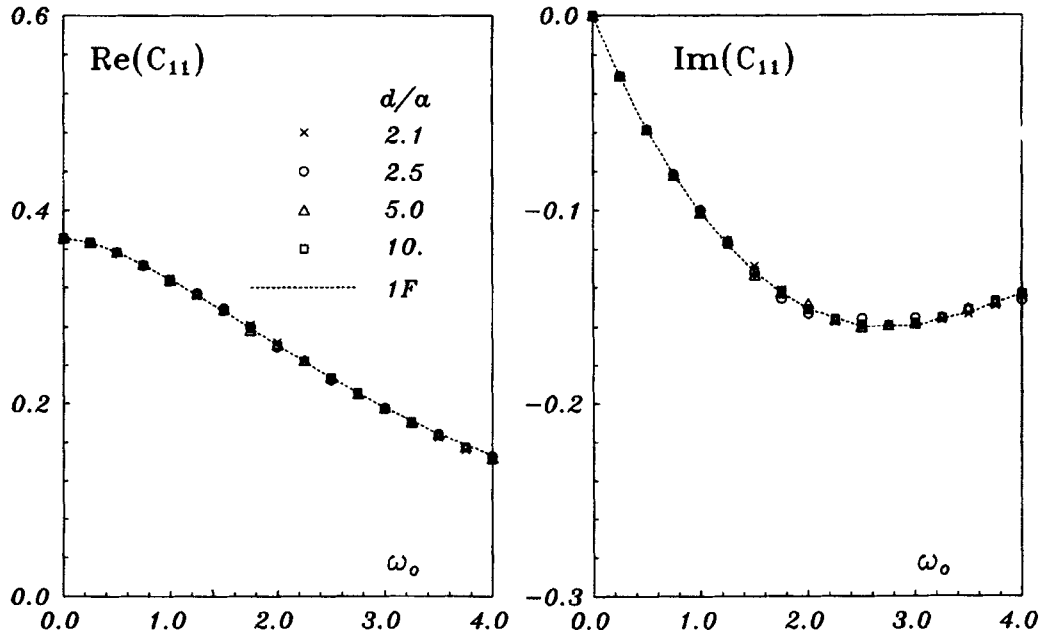

Figure 8. Effects of footing separation on the vertical compliance of the active footing, for $E = 0{\cdot}02431$

footing at the centre point. It is found that the difference between soft and stiff footings is not as significant as in the case of a centre point load. The coupling compliance functions of the passive footing are shown in Figure 13 for three values of separation distance $d/a = 2{\cdot}5$, $5{\cdot}0$, $10{\cdot}0$. Unlike the case of point loading, coupling effects between active and passive footings under a uniform distributed load decay rapidly at higher frequencies for either stiff or soft footings.

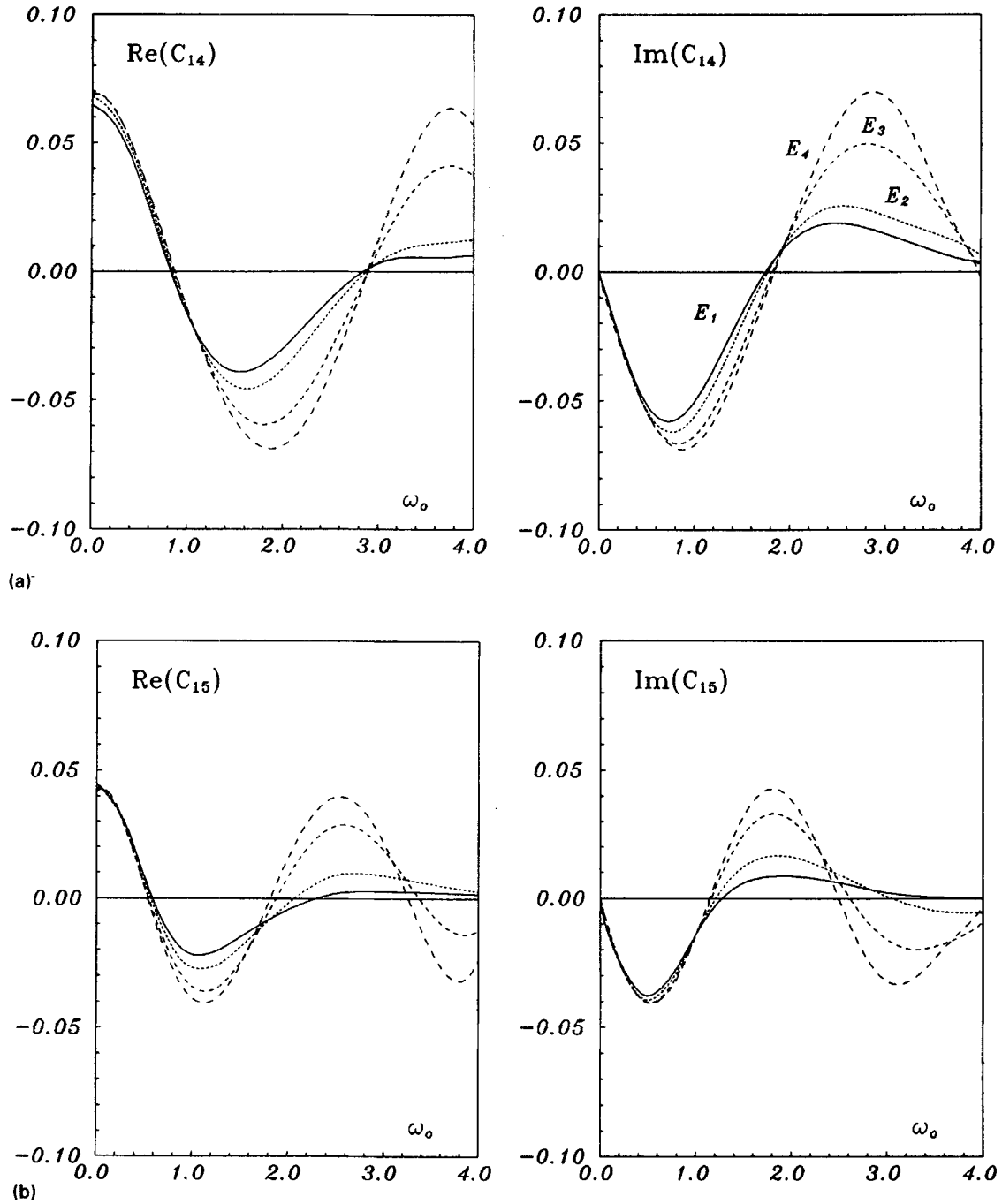

Figure 9. Coupling vertical compliance of the passive footing at (a) mid-point of the near edge, No. 4, (b) the centre, and (c) mid-point of the far edge, No. 6 for footing separation $d/a = 2{\cdot}50$: (———) E_1; (· · · · ·) E_2; (– – – –) E_3; (— — — —) E_4

5. A CASE STUDY OF THE TRANSIENT RESPONSE BY INVERSE TRANSFORMATION

The dynamic compliance coefficient in the time domain can be generally determined directly through a Fourier inverse transformation from the corresponding frequency domain formulation given in previous sections. In general, the transformation from the frequency to the time domain has to be performed

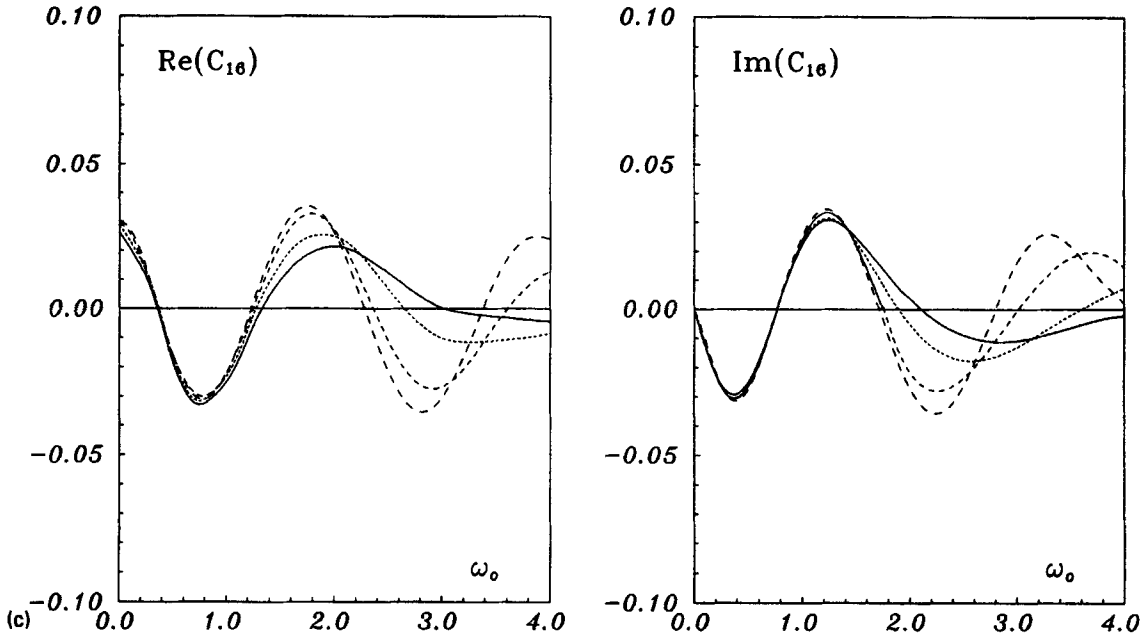

Figure 9. *Continued.*

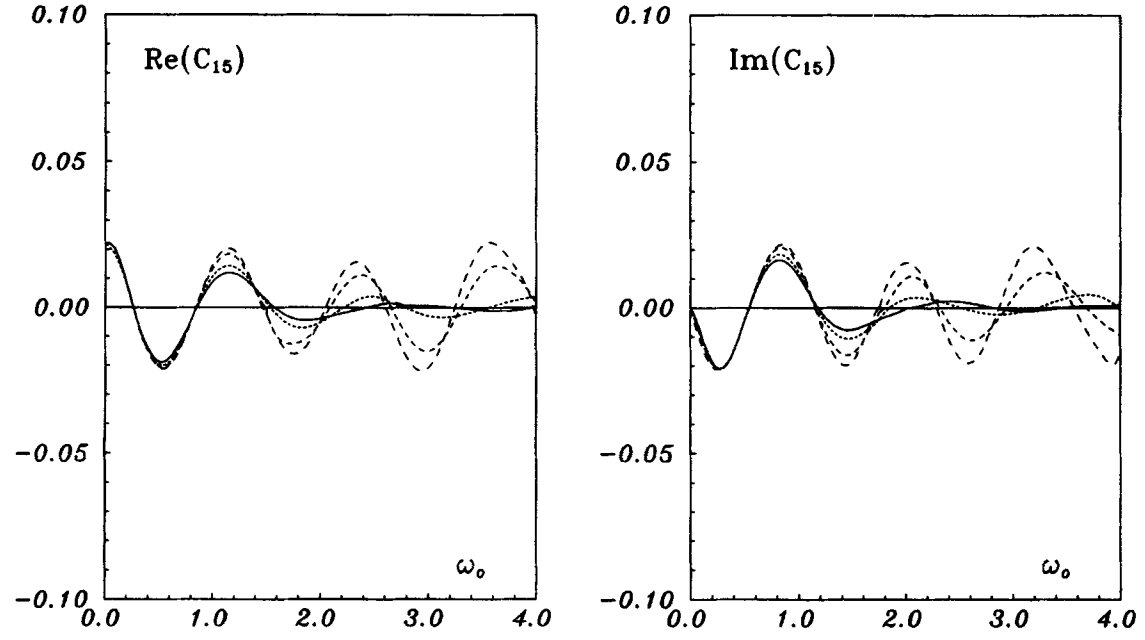

Figure 10. Coupling vertical compliance of the passive footing, for footing separation $d/a = 5{\cdot}00$: (———) E_1; (· · · · ·) E_2; (– – – –) E_3; (— — —) E_4

numerically. As equations (2) and (8) represent unit-impulse response of the footing system, the transient response due to a general time-varying force $p(t)$ can be obtained by using the convolution integral of the unit-impulse response

$$\{u(t)\} = \frac{1}{\sqrt{2\pi}} \int_{-\infty}^{+\infty} \left[\int_0^t p(\tau) e^{i\omega\tau} d\tau \right] \{U(\omega)\} e^{-i\omega\tau} d\omega \tag{10}$$

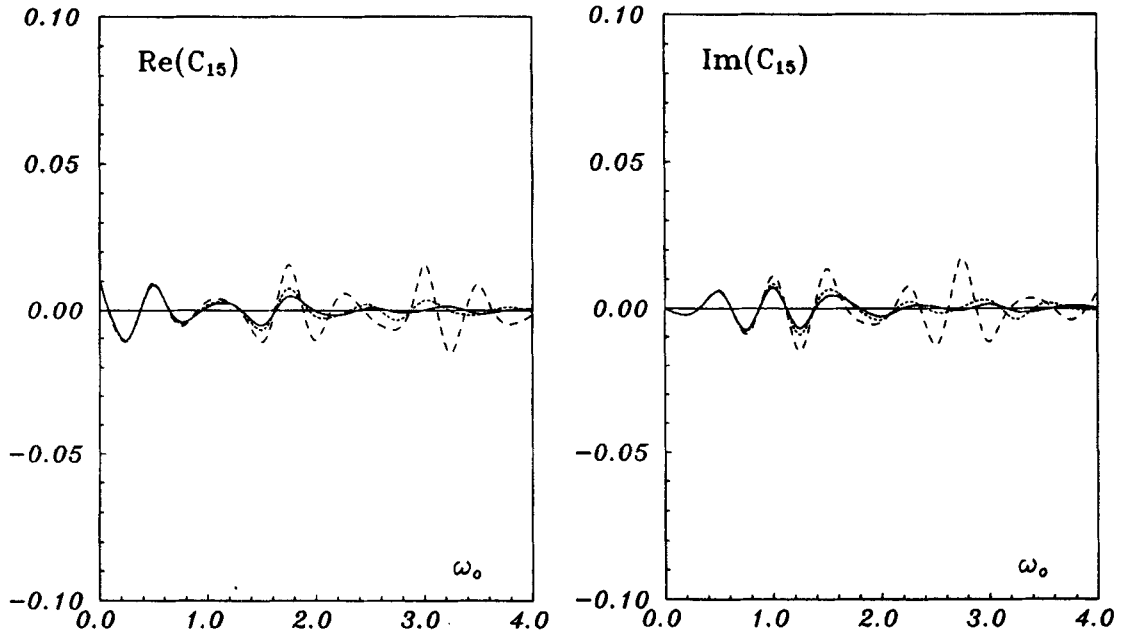

Figure 11. Coupling vertical compliance of the passive footing, for footing separation $d/a = 10{\cdot}0$: (———) E_1; (· · · · ·) E_2; (— — —) E_4

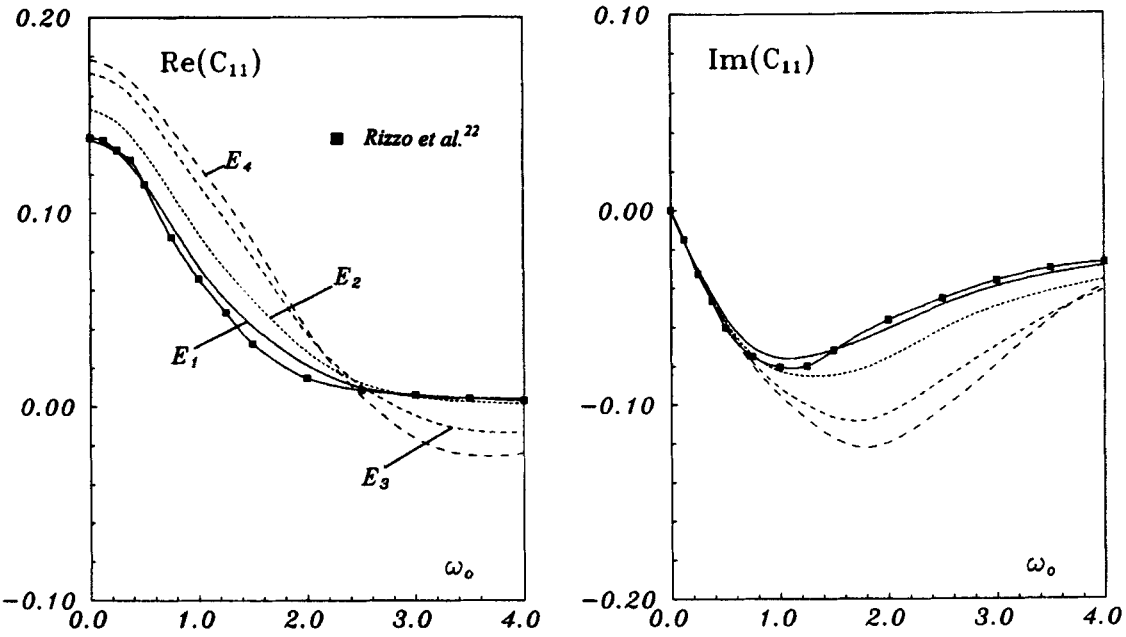

Figure 12. Vertical compliance of the active footing due to a uniformly distributed load, for footing separation $d/a = 2{\cdot}50$

Numerical computation is carried out for a two-footing system, shown in Figure 6, subjected to a suddenly applied, uniformly distributed vertical force of magnitude p_0. Geometrical parameters and material properties of the footing system are chosen as $a = 25$ m, $h = 2{\cdot}5$ m, $d = 62{\cdot}5$ m, $v_s = 1/3$, $v_f = 0{\cdot}3$, $E_f = 35$ GPa and $E_s = 20$ MPa. The dimensionless time is defined as $\bar{t} = c_s t/a$. The inverse transformation is performed over

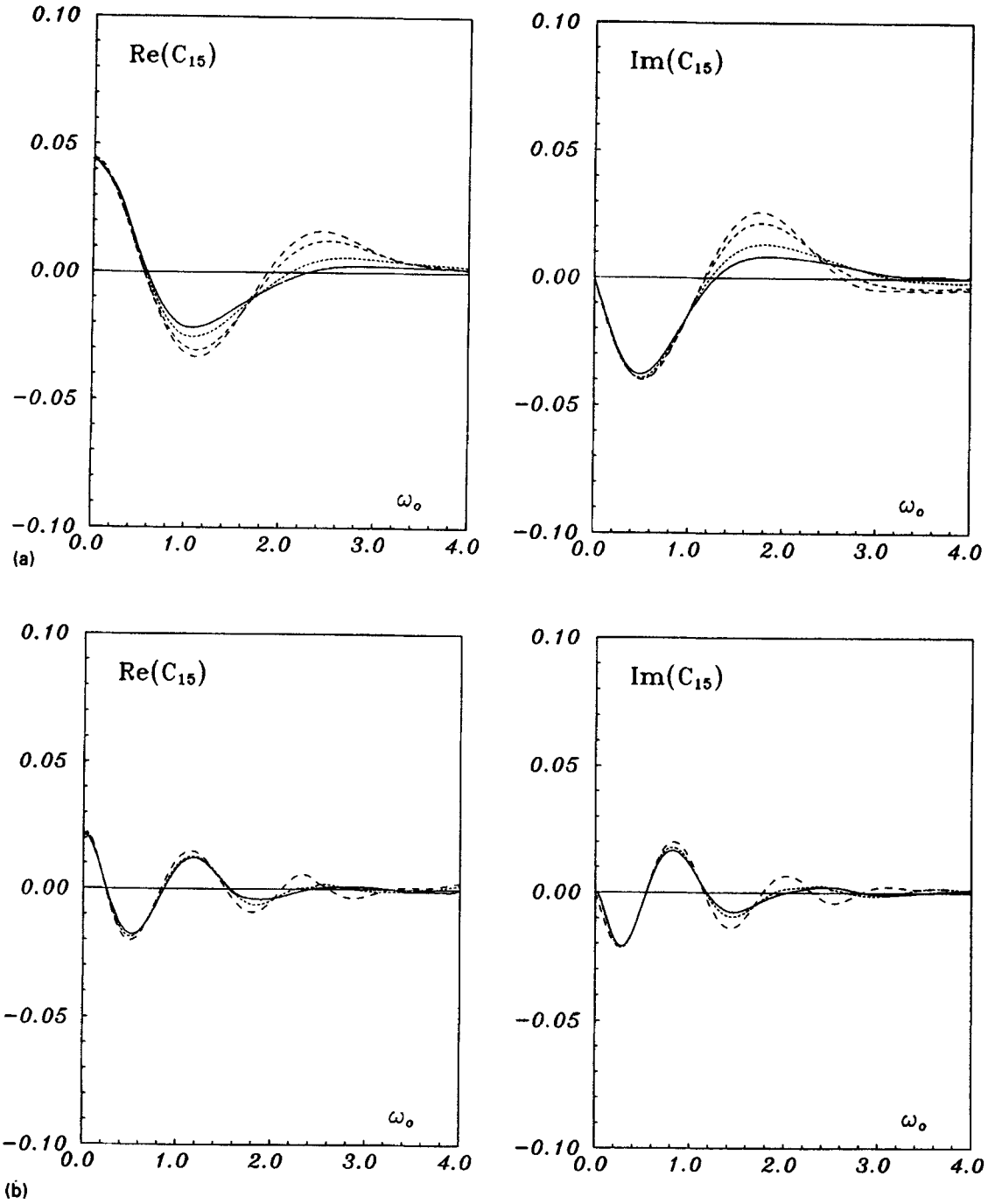

Figure 13. Coupling vertical compliance of the passive footing due to a uniformly distributed load; for (a) footing separation $d/a = 2{\cdot}50$, (b) footing separation $d/a = 5{\cdot}00$, and (c) footing separation $d/a = 10{\cdot}0$: (———) E_1; (· · · · ·) E_2; (– – – –) E_3; (— — —) E_4

a frequency span up to $a_0 = 10$ and with increment $\Delta a_0 = 0{\cdot}02$. It can be seen that error due to the cut-off of high frequency will be of the order of $O(a_0^{-2})$. Figure 14 shows the vertical displacement, $\bar{W}_i = W_i E_s / 2a(1 + v_s)\, p_0$ at the centre of the active footing versus dimensionless time while Figure 15 presents the vertical displacement at the centre of the passive footing. Figure 15 clearly shows that the suddenly

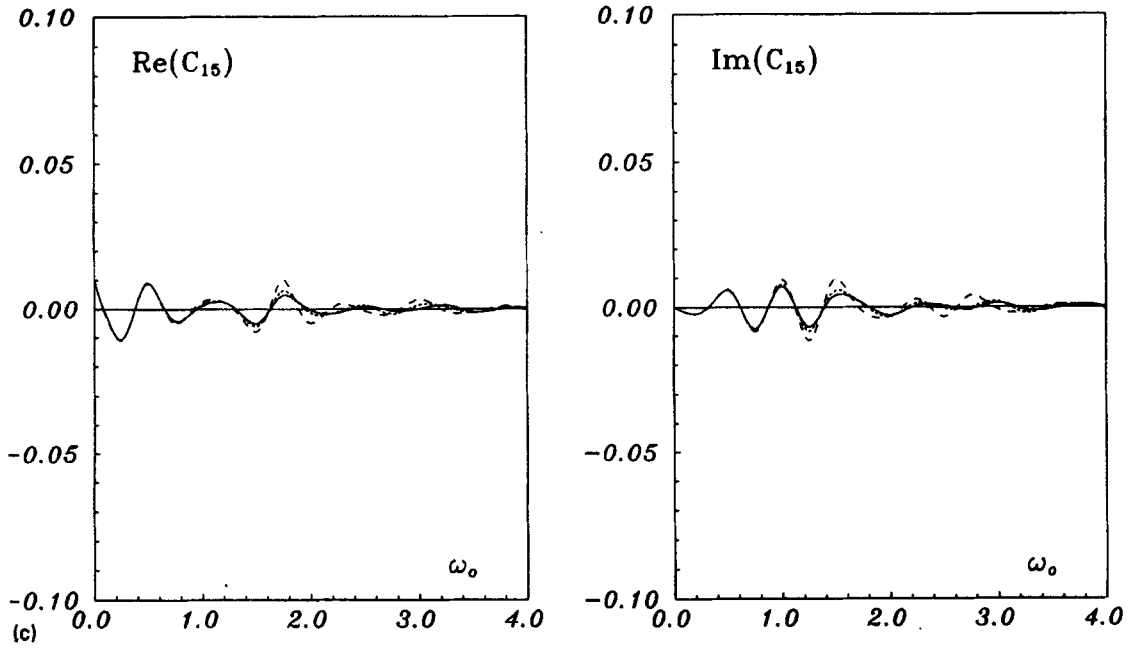

Figure 13. *Continued.*

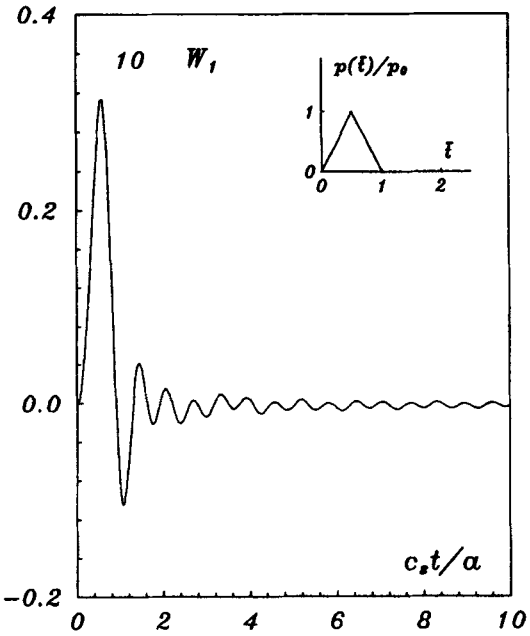

Figure 14. Vertical transient response of the active footing

applied load causes the passive footing to start moving with an acceleration in the direction opposite to that of the applied force. The response magnitude of the passive footing is only about 1 per cent in comparison with that of the active one but continues for a longer time interval.

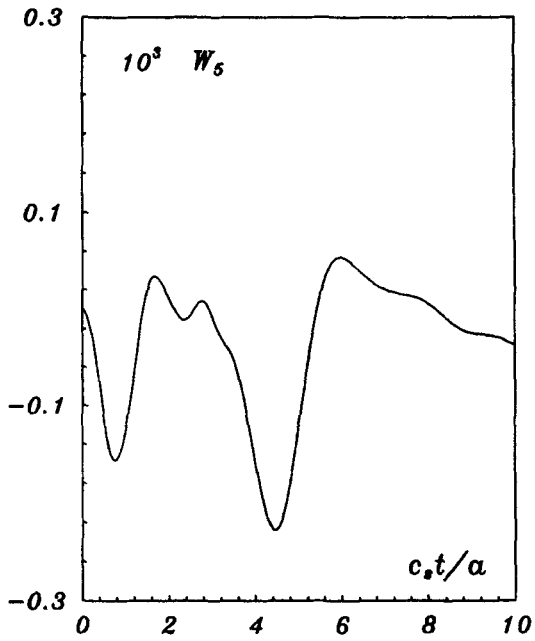

Figure 15. Vertical transient response of the passive footing

6. CONCLUSIONS

An accurate and efficient numerical procedure for the dynamic response analysis of flexible surface footings of arbitrary geometries subjected to either harmonic or transient external forces has been presented. The method employs quadratic isoparametric elements to discretize the surface of the half-space as well as the flexible footing, and has advantages not only with respect to its rapid convergence and ability to accommodate complicated geometry but also for its full compatibility of displacements and stresses at the contact interfaces.

In the case of a single footing, it has been found that the response of the footing depends on the distribution of the applied load if the footing is fairly flexible. It is also observed that the 'active' footing of a two-footing system behaves similarly. On the other hand, the 'passive' footing of the system seems to be insensitive to the load distribution in the low-frequency range, though the influence may become considerable as the frequency increases. The results also indicate that the existence of the 'passive' footing has very little effect on the behaviour of the 'active' footing. Conversely, the behaviour of the 'passive' footing is affected by the 'active' footing and depends considerably on the separation between the two footings and the applied load. In particular, for the system with fairly flexible footings under a point load, displacements induced in the 'passive' footing may be significant over quite a large range of frequency while it decays rapidly for a stiff footing. In the case of uniformly distributed load, the coupling effects between the footings decay rapidly at high frequency irrespective of the stiffness of the footings. In the case of the two-footing system under the action of a load applied suddenly to one of the footings, the response of the 'active' footing may be significant during the loading period, while the response of the 'passive' footing, though quite small in magnitude, may continue several times longer than the loading period.

ACKNOWLEDGEMENT

The financial supports of the Croucher Foundation and the University Research Grants Council are acknowledged.

APPENDIX

The surface half-space Green's function can be determined by using a double Fourier transformation with respect to coordinate variables x and y and has the form

$$G_{11}(r,\phi) = \frac{1}{2\pi\mu r}\int_0^{+\infty}\left[\frac{k_2^2 r^2 f(r)}{F(z,k_2)}\cos^2\phi - \frac{\sin^2\phi}{f(r)}\right] zJ_0(z)\,dz$$
$$-\frac{\cos 2\phi}{2\pi\mu r}\int_0^{+\infty}\left[\frac{k_2^2 r^2 f(r)}{F(z,k_2)} + \frac{1}{f(r)}\right] J_1(z)\,dz$$

$$G_{12}(r,\phi) = G_{21}(r,\phi) = \frac{\sin 2\phi}{2\pi\mu r}\int_0^{+\infty}\left[\frac{k_2^2 r^2 f(r)}{F(z,k_2)} + \frac{1}{f(r)}\right]\left[\frac{z}{2}J_0(z) - J_1(z)\right] dz$$

$$G_{13}(r,\phi) = -G_{31}(r,\phi) = \frac{\cos\phi}{2\pi\mu r}\left[\frac{1}{2} + \int_0^{+\infty}\frac{k_2^2 r^2 f^*(r)}{F(z,k_2)}\,J_1(z)\,dz\right]$$

$$G_{22}(r,\phi) = \frac{1}{2\pi\mu r}\int_0^{+\infty}\left[\frac{k_2^2 r^2 f(r)}{F(z,k_2)}\sin^2\phi - \frac{\cos^2\phi}{f(r)}\right] zJ_0(z)\,dz$$
$$+\frac{\cos 2\phi}{2\pi\mu r}\int_0^{+\infty}\left[\frac{k_2^2 r^2 f(r)}{F(z,k_2)} + \frac{1}{f(r)}\right] J_1(z)\,dz$$

$$G_{23}(r,\phi) = -G_{32}(r,\phi) = \frac{\sin\phi}{2\pi\mu r}\left[\frac{1}{2} + \int_0^{+\infty}\frac{k_2^2 r^2 f^*(r)}{F(z,k_2)}\,J_1(z)\,dz\right]$$

$$G_{33}(r,\phi) = \frac{1}{2\pi\mu r}\int_0^{+\infty}\frac{k_2^2 r^2 f^{**}(r)}{F(z,k_2)}\,zJ_0(z)\,dz$$

where $J_0(z)$ and $J_1(z)$ are the Bessel's function of the first kind of order 0 and 1, respectively, and

$$F(z,k_2) = (2z^2 - k_2^2 r^2)^2 - 4z^2 f(r) f^{**}(r)$$
$$f(r) = (z^2 - k_2^2 r^2)^{1/2}$$
$$f^*(r) = (z^2 - k_2^2 r^2/2)$$
$$f^{**}(r) = [z^2 - (c_2^2/c_1^2)k_2^2 r^2]^{1/2}$$

and $k_2 = \omega/c_2$, ω is the circular frequency, $c_1 = [(\lambda + 2\mu)/\rho]^{1/2}$ and $c_2 = [\mu/\rho]^{1/2}$ are the dilational and shear wave velocities, respectively, with λ and μ being the Lame's elastic constants and ρ the mass density; r is the distance from the observer $(x, y, 0)$ to the receiver $(x_p, y_p, 0)$, ϕ is the angle between vector r and the x axis.

REFERENCES

1. G. B. Warburton, J. D. Richardson and J. J. Webster, 'Forced vibration of two masses on an elastic half space', *J. appl mech. ASME* **38**, 148–156 (1971).
2. J. Dominguez, 'Dynamic stiffness of rectangular foundations', *Report No. R78–20*, Department of Civil Engineering, Massachusetts Institute of Technology, Cambridge, MA, 1978.
3. J. E. Luco, 'Linear soil-structure interaction: a review', in S. K. Datta (eds) *Earthquake Ground Motion and its Effects on Structures*, ASME, New York, 1982, pp. 41–57.
4. D. E. Beskos, 'Applications of the boundary element method in dynamic soil–structure interaction', in P. Gulkan and R. W. Clough (eds), Kluwer Academic Publishers, Dordrecht, 1993, pp. 61–90.
5. J. Qian and D. E. Beskos, 'Dynamic interaction between 3-D rigid surface foundations and comparison with the ATC-3 provisions', *Earthquake eng. struct. dyn.* **24**, 419–437 (1995).
6. M. Iguchi and J. E. Luco, 'Vibration of flexible plate on viscoelastic medium', *J. eng. mech. div. ASCE* **108**, 1103–1120 (1982).
7. M. Iguchi and J. E. Luco, 'Dynamic response of flexible rectangular foundations on an elastic half-space', *Earthquake eng. struct. dyn.* **9**, 239–249 (1981).
8. M. A. Oien, 'Steady motion of a plate on an elastic half space', *J. appl. mech. ASME*, **40**, 478–484 (1973).
9. C. C. Spyrakos and D. E. Beskos, 'Dynamic response of flexible strip foundations by boundary and finite elements', *Soil dyn. earthquake eng.* **5**, 84–96 (1986).

10. S. A. Savidis and T. Richter, 'Dynamic response of elastic plates on the surface of the half-space', *Int. j. numer. anal. methods geomech.* **3**, 245–254 (1979).
11. W. L. Whittaker and P. Christiano, 'Response of a plate and elastic half-space to harmonic waves', *Earthquake eng. struct. dyn.* **10**, 255–266 (1982).
12. W. L. Whittaker and P. Christiano, 'Dynamic response of plate on elastic half-space', *J. eng. mech. div. ASCE*, **108**, 133–154 (1982).
13. D. L. Karabalis, C. C. Spyrakos and D. E. Beskos, 'Dynamic response of surface foundations by time domain boundary element method' in D. E. Beskos *et al.* (eds) *Dynamic Soil-Structure Interaction*, A. A. Balkema, Rotterdam, 1984, pp. 19–24.
14. D. L. Karabalis and D. E. Beskos, 'Dynamic response of 3-D flexible foundations by time domain BEM and FEM', *Soil dyn. earthquake eng.* **4**, 91–101 (1985).
15. Y. J. Lin, 'Dynamic response of circular plates resting on visco-elastic half space', *J. appl. mech. ASME* **45**, 379–384 (1978).
16. S. Kren and H. Schmidt, 'Vibration of an elastic circular plate on an elastic half space – a direct approach', *J. appl. mech. ASME*, **48**, 161–168 (1981).
17. R. K. N. D. Rajapakse, 'Dynamic response of elastic plates on visco-elastic half space', *J. eng. mech. ASCE* **115**, 1867–1881 (1989).
18. Y. Wang, R. K. N. D. Rajapakse and A. H. Shah, 'Dynamic interaction between flexible strip foundations', *Earthquake eng. struct. dyn.* **20**, 441–454 (1991).
19. O. J. Svec, 'Thick plates on elastic foundations by finite elements', *J. eng. mech. div. ASCE* **102**, 461–477 (1976).
20. R. K. N. D. Rajapakse and A. P. S. Selvadurai, 'On the performance of Mindlin plate elements in modelling plate-elastic medium interaction: a comparative study', *Int. j. numer methods eng.* **23**, 1229–1244 (1986).
21. G. D. Manolis and D. E. Beskos, *Boundary Element methods in Elasto-dynamics*. Unwin Hyman, London, 1988.
22. F. J. Rizzo, D. J. Shippy and M. Rezayat, 'Boundary integral equation analysis for a class of earth-structure interaction problems', *Final Report NSF CEE*-8013461, Engineering Mechanics Department, University of Kentucky, Lexington, KY, 1985.
23. Y. K. Cheung and Zienkiewicz, 'Plates and tanks on elastic foundations–an application of finite element method', *Int. j. solids struct.* **1**, 451–461 (1965).